IFAC

Adaptive Optimal Path Following
for High Wind Flights

Ashwini Ratnoo * P.B. Sujit ** Mangal Kothari ***

** Postdoctoral Fellow, Department of Aerospace Engineering,
Technion-Israel Institute of Technology, Haifa, 32000, Israel. (email:
ashwini@aerodyne.technion.ac.il)*
*** Research Scientist, Department of Electrical and Computer
Engineering, University of Porto, Portugal - 4200-395. (email:
sujit@fe.up.pt)*
**** Graduate student, Department of Engineering, University of
Leicester, United Kingdom-LE1 7RH. (email: mk221@le.ac.uk)*

Abstract: Unmanned aerial vehicle path following is addressed as an infinite horizon regulator problem. Using the linear quadratic regulator technique an optimal guidance law is derived. The state weighting matrix is chosen as a function of the position error and this adaptive nature of the cost function controls the UAV errors tightly. Numerical simulations are carried out for straight line and circular paths under various wind conditions. Results show considerably lower position errors as compared to an existing guidance law. Path following with winds up to half the vehicle airspeed is achieved.

Keywords: Guidance systems, Optimal control, Path planning

1. INTRODUCTION

Unmanned aerial vehicles (UAVs) have been successfully deployed in various applications that include search and rescue, surveillance, patrol and monitoring missions. They have the capability to provide information remotely and act like an extended sensor. With advances in flight control and miniaturization of UAVs, they are found to play a key role in urban environments. Of particular interest is path following in high winds. Urban environments have unstructured wind patterns and with high magnitudes causing very high errors in UAV path following. Most of the mission paths can be defined using a set of way-point and loiters maneuvers, where way-points are straight line segments while loiters are circular orbits. The path following controller has to accurately track the desired path in presence of wind disturbances. The path following control law must have low computational complexity to be used in real-time.

There is wide body of literature on developing guidance laws for UAVs to follow straight line, curved trajectories and loiter maneuvers in the presence of winds. A piecewise-affine control law with Lyapunov based controller for the UAV to follow a path is presented by Shehab and Rodrigues [2005]. The authors did not consider wind disturbances in their work. Kaminer et al. [2006] developed an optimal control law for multiple UAV trajectory following with coordination. The trajectory is parameterized as a function of time to follow which becomes an issue when UAV is initially located away from the path. A $\mathcal{L}_1$ adaptive controller for UAV path following taking wind disturbances into account is developed by Cao et al. [2007]. Nelson et al. [2006] developed a simple and effective path following controller using vector fields. Vector fields are developed for both straight line and circular paths in the presence of winds. Rysdyk [2006] developed guidance laws for following straight line and circular paths based on helmsman behavior. The guidance law changes the course of the vehicle based on the wind magnitude and direction which is estimated online. Lawrence et al. [2006] developed a generalized vector field method with lyapunov stability for different maneuvers. Ceccarelli et al. [2007] designed a guidance law for a MAV taking wind into consideration for continuous monitoring a target in the camera field of view. Breivik and Fossen [2007] presented guidance laws for path following in 2D and 3D using control lyapunov functions. The approach does not take wind into account. Park et al. [2007] presented a non-linear guidance law (NLGL) that generates a reference target point on the path and uses this reference point as a target to maneuver the aircraft along the path. The authors present theoretical results and show results through experiments under wind disturbances.

A typical path following command as a constant gain linear function of position and velocity errors is incapable of placing a hard bound on the position error. As the main contribution of the present work, we present an optimal UAV path following guidance law as an infinite horizon linear quadratic regulator (LQR) solution with an adaptive running cost where the state weighting gains are functions of the position error itself. The state weighting matrix is chosen as a function of the current and the maximum allowable position error and this adaptive nature of the cost function controls the UAV errors tightly in presence of winds. The guidance law does not require path curvature information and is based on position and heading errors of the UAV.

The organization of the rest of the paper is as follows: The UAV path following problem is defined in Section 2 followed by the adaptive optimal guidance law derivation in Section 3. Guidance law implementation and UAV kinematics are described in Section 4. Section 5 presents the simulations studies on the guidance laws with comparative results. Section 6 contains concluding remarks.
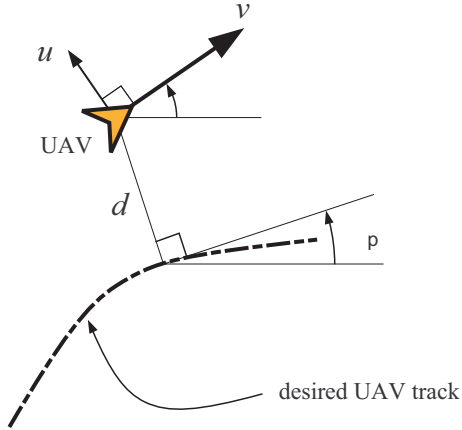
2. PROBLEM FORMULATION

Fig. 1. Formulation Geometry

Consider a UAV flying with a constant speed v in a plane as shown Fig. 1. The UAV mission is to follow a desired path as shown with the dashed line in Fig. 1. The UAV has a position error of d with respect to the desired path and also a velocity error calculated as

$$\dot{d} = v \sin{(\psi - \psi_p)} \tag{1}$$

where v, ψ and ψ_p are the UAV speed, heading angle, and desired path angle, respectively. The path following problem is to formulate a control law u for the UAV to keep the errors, d and $\dot{d}$ small in presence of changing desired path geometries and winds. We consider the path following problem with a bound on the allowable error as

$$|d| \leq d_b \tag{2}$$

where $|d_b|$ is the desired position error band with respect to the path. Also, u is the lateral acceleration which can be related to the UAV heading angle rate $\dot{\psi}$, as

$$u = v\dot{\psi} \tag{3}$$

3. ADAPTIVE OPTIMAL GUIDANCE LAW

The problem of UAV path following is inherently an infinite horizon regulator problem where the guidance objective is to annul the UAV position and velocity errors with respect to a desired path. Contrary to finite time missile guidance applications, the UAV regulator solutions should keep the errors close to zero for all times and not just at the termination of the flight. We use adaptive running cost on the error states in an infinite horizon regulator formulation for the UAV path following problem.

3.1 Infinite horizon LQR

Consider the general infinite-horizon nonlinear regulator problem of the form:
Minimize

$$J = \frac{1}{2} \int_{t_0}^{\infty} [x^T Q x + R u^2(t)] dt \tag{4}$$

with respect to the state x and control u subject to the linear system dynamics

$$\dot{x} = Ax + Bu \tag{5}$$

and derive the feedback control

$$u^* = -R^{-1} B^T P x \tag{6}$$

where P is obtained from the algebraic Riccati equation

$$A^T P + P A - P B R^{-1} B^T P + Q = 0 \tag{7}$$

and $Q \geq 0$ and $R > 0$ are design parameters.

3.2 Trajectory Tracking Problem and LQR Solution

Linearizing UAV dynamics with respect to the desired heading as

$$v_d = \dot{d} = v \sin{(\psi - \psi_p)} \tag{8}$$
$$\dot{v}_d = v(\dot{\psi} - \dot{\psi}_p) \cos{(\psi - \psi_p)} \tag{9}$$

In the absence of path curvature information, we assume $\dot{\psi}_p = 0$. Using (3) and substituting for $\dot{\psi}_p$ in (9) with small angle $(\psi - \psi_p) \rightarrow 0$, we have

$$\dot{v}_d = v\dot{\psi} = u \tag{10}$$

Representing (8) and (10) in the standard form

$$\dot{\mathbf{x}} = \mathbf{A}\mathbf{x} + \mathbf{B}u \tag{11}$$

we have

$$\mathbf{x} = \begin{bmatrix} d \\ v_d \end{bmatrix}, \ \mathbf{A} = \begin{bmatrix} 0 & 1 \\ 0 & 0 \end{bmatrix}, \ \mathbf{B} = \begin{bmatrix} 0 \\ 1 \end{bmatrix} \tag{12}$$

Consider the general infinite-horizon linear quadratic regulator problem where we minimize

$$J = \frac{1}{2} \int_{t_0}^{\infty} [\mathbf{x}^T \mathbf{Q} \mathbf{x} + R u^2(t)] dt \tag{13}$$

with respect to $\mathbf{x}$ and u subject to (11). Here, $\mathbf{Q}$ and R are the state weighting matrix and the control weighting matrix, respectively. Also, $\mathbf{Q}$ and R are the two design parameters available to us for obtaining the desired control. We assume

$$R = 1 \tag{14}$$

and $\mathbf{Q}$ to be an adaptive matrix with

$$\mathbf{Q} = \begin{bmatrix} q_1^2 & 0 \\ 0 & q_2^2 \end{bmatrix} \geq 0 \tag{15}$$

We check the conditions for the LQR control solution to be locally asymptotically stable as,

(1) $\{\mathbf{A}, \mathbf{B}\}$ should be controllable in the domain of interest.
Using (12) we have,

$$|\{\mathbf{B}, \mathbf{A}\,\mathbf{B}\}| = -1 \neq 0 \qquad (16)$$

(2) $f(\mathbf{x}) = \mathbf{A}\mathbf{x} \in C^1$.
From (12), we deduce

$$\mathbf{A}\mathbf{x} = \begin{bmatrix} d \\ 0 \end{bmatrix} \in C^1 \qquad (17)$$

(3) $f(0) = 0$.
Using (17), we have

$$f(0) = \begin{bmatrix} 0 \\ 0 \end{bmatrix} \qquad (18)$$

(4) $\mathbf{B} \neq \mathbf{0}$.
From (12) we have $\mathbf{B}$ as a constant non-zero matrix.
(5) $\mathbf{Q} \geq 0$ and $R > 0$.
From (15) and (14) these conditions are met.

Solving algebraic Riccati equation   Optimal solution for the optimal control problem (13) is given as,

$$u^* = -R^{-1}\mathbf{B}^T\mathbf{P}x \qquad (19)$$

where $\mathbf{P} > 0$ is defined as,

$$\mathbf{P} = \begin{bmatrix} p_{11} & p_{12} \\ p_{12} & p_{22} \end{bmatrix} \qquad (20)$$

is obtained by solving the algebraic Riccati equation,

$$\mathbf{A}^T\mathbf{P} + \mathbf{P}\mathbf{A} - \mathbf{P}\mathbf{B}\mathbf{R}^{-1}\mathbf{B}^T\mathbf{P} + \mathbf{Q} = 0 \qquad (21)$$

Solving for $\mathbf{P}$ using (12), (14), (15) and (20) in (21), we have

$$\begin{bmatrix} 0 & 0 \\ 1 & 0 \end{bmatrix}\begin{bmatrix} p_{11} & p_{12} \\ p_{12} & p_{22} \end{bmatrix} + \begin{bmatrix} p_{11} & p_{12} \\ p_{12} & p_{22} \end{bmatrix}\begin{bmatrix} 0 & 1 \\ 0 & 0 \end{bmatrix} - \begin{bmatrix} p_{11} & p_{12} \\ p_{12} & p_{22} \end{bmatrix}\begin{bmatrix} 0 \\ 1 \end{bmatrix}$$
$$\times \begin{bmatrix} 0 & 1 \end{bmatrix}\begin{bmatrix} p_{11} & p_{12} \\ p_{12} & p_{22} \end{bmatrix} + \begin{bmatrix} q_1^2 & 0 \\ 0 & q_2^2 \end{bmatrix} = 0 \qquad (22)$$

Simplifying and equating individual elements, we have,

$$p_{12} = q_1 \qquad (23)$$

$$p_{22} = \sqrt{2q_1 + q_2^2} \qquad (24)$$

$$p_{11} = q_1\sqrt{2q_1 + q_2^2} \qquad (25)$$

Adaptive feedback control   Using (12), (20), (23), (24) and (25) in (19), we have the optimal control solution as,

$$u^* = -\begin{bmatrix} 0 & 1 \end{bmatrix}\begin{bmatrix} p_{11} & p_{12} \\ p_{12} & p_{22} \end{bmatrix}\begin{bmatrix} d \\ v_d \end{bmatrix}$$
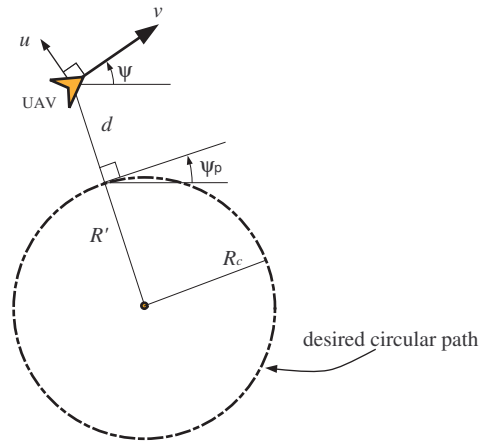$$= -\left[q_1\,d + \sqrt{+2q_1 + q_2^2}\,v_d \right] \qquad (26)$$

We propose an adaptive gain q_1^2 for a running penalty on d as,

$$q_1^2 = \left| \frac{d_b}{d_b - d} \right| \qquad (27)$$

where d_b is the maximum allowable position error as considered in (2). The adaptive state weight q_1 increases
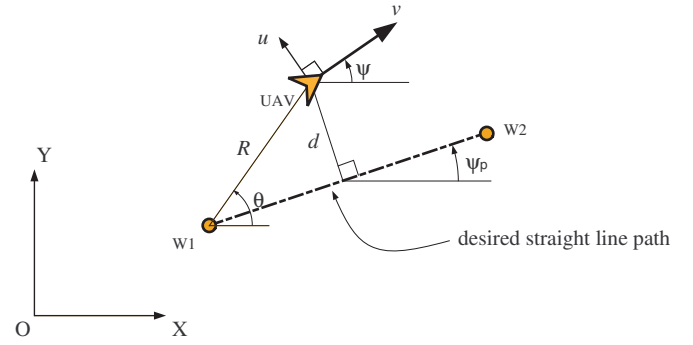
(a) Straight-line

(b) Circular

Fig. 2. Path geometries

the penalty as the UAV position error increases and gets closer to the maximum allowable limit. Very close to the maximum allowable limit the UAV uses maximum control to keep itself in the desired error band. Note that, the weight remains close to unity for UAV flights with negligible error d. This way the error d is controlled tightly in case there are sudden changes in the desired path or wind disturbances. Since there are no practical concerns on the gain q_2^2 associated with v_d, we chose

$$q_2^2 = 1 \qquad (28)$$

Using (27) and (28) in (26), we have the adaptive optimal guidance law (AOGL) as

$$u^* = -\left[\sqrt{\left|\frac{d_b}{d_b - d}\right|}\, d + \sqrt{2\sqrt{\left|\frac{d_b}{d_b - d}\right|} + 1}\, v_d \right] \qquad (29)$$

4. GUIDANCE LAW IMPLEMENTATION

UAV trajectory planning involves two standard geometries, namely, the straight line/way-point guidance and circular/loiter guidance. The guidance law of (29) can be implemented on the two standard geometries and the related kinematics are described next.

4.1 Straight-line following

Consider a straight line path formed by the way-points W1-W2 as shown in Fig. 2 (a). Let R be the displacement of UAV with respect to point W1 making an angle θ with the reference. The UAV position and velocity errors can be calculated as,

$$d = R \sin (\theta - \psi_p) \tag{30}$$

and

$$\dot{d} = v \sin (\psi - \psi_p), \tag{31}$$

respectively.

4.2 Circular path following

Consider a circular path of radius R_c as shown in Fig. 2 (b). Let R' be the displacement of the UAV with respect to the center of the circular path. The UAV position and velocity errors can be calculated as,

$$d = R' - R_c \tag{32}$$

and

$$\dot{d} = v \sin (\psi - \psi_p), \tag{33}$$

4.3 Effect of wind

Motion of a UAV with respect to ground or stationary desired paths is affected by wind disturbances. In presence of wind the ground velocity components, say v_{gx} and v_{gy}, of the UAV are given as

$$v_{gx} = v \cos \psi + v_{wx} \tag{34}$$

$$v_{gy} = v \sin \psi + v_{wy} \tag{35}$$

where v_{wx} and v_{wy} are the components of the wind speed v_w along X and Y direction. Note that though d is independent of wind, v_d in presence wind can be expressed as

$$v_d = v \sin (\psi - \psi_p) + v_w \sin (\psi_w - \psi_p) \tag{36}$$

where ψ_w is the direction of wind with reference.
Note that kinematics described in this section is used to simulate trajectories in the next section. However, in real life scenarios a GPS/INS aided UAV can compute onboard its ground position and ground velocity and then d and v_d can directly be computed with respect to any path.

5. SIMULATION RESULTS

Using the guidance law derived in (29) we simulate various path following scenarios. Simulations are carried out for straight line and circular paths considering the two as the basic geometries for a general path planning problem. For comparative studies we use well known non-linear guidance law (NLGL)Park et al. [2007] and present the results here. The UAV speed, v, is considered 25 m/sec with a minimum turn radius $r_{min} = 3v = 75$ m.
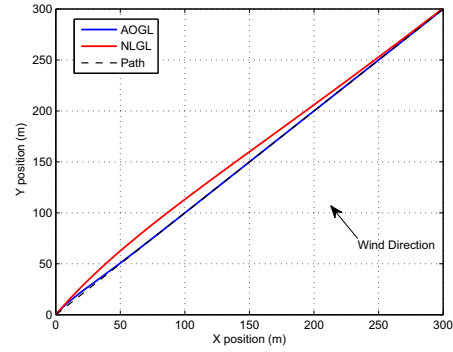
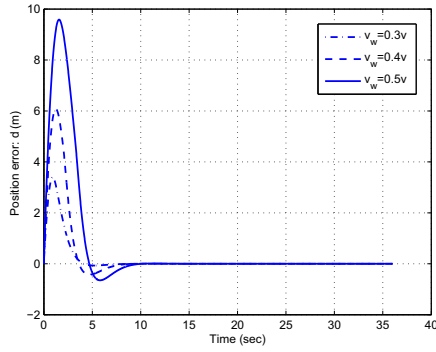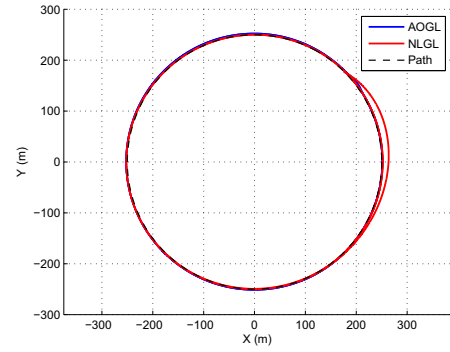(a) Trajectories
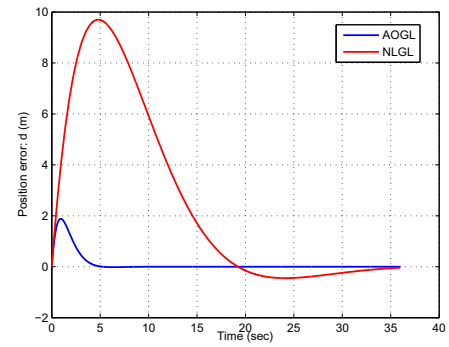
(b) Position error
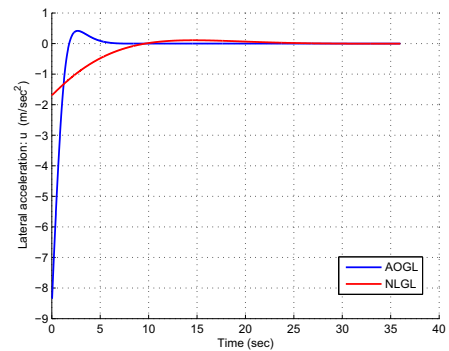
(c) Lateral accelerations

Fig. 3. Straight line following in 20% wind
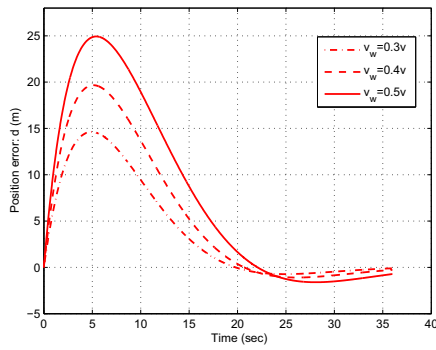
5.1 Straight line following

Consider a straight line path passing through the origin of the X-Y plane with a unity slope as shown by a dashed line in Fig. 3(a) with a dashed black line. We consider wind with $v_w = 0.2v$ blowing perpendicular to the desired path with $\psi_w = 135°$. The parameters used for AOGL are: $d_b = 4$ and for NLGL - $L1 = 150$. Trajectories for AOGL and NLGL are plotted in Fig.3 (a) with blue and red colors, respectively. The NLGL trajectory is affected highly by the cross wind. The corresponding position errors are shown Fig. 3(b) where AOGL has a maximum UAV position error of 2 m and the transient of the position error settles quickly to the steady state. Whilst NLGL has a maximum position error is as high as 9.5 m and the guidance law has much higher settling time. Lateral acceleration profiles for
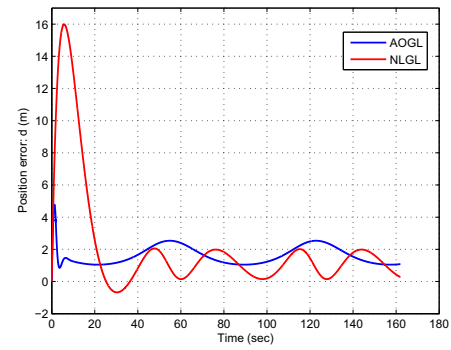
(a) Position error for AOGL

(b) Position error for NLGL

Fig. 4. Position error comparison in 30, 40 and 50 % wind following a straight line path

the case are plotted in Fig. 3(c). For AOGL, as shown in blue color, the adaptive gains of (29) quickly increase as the wind induces the position error. This higher control input quickly reduces the position error and both the errors and the control input go to zero at a fast rate . The NLGL lateral acceleration is lower initially resulting in a higher position error caused due to wind. Further, we vary the wind speed magnitude and compare the performance of the two guidance laws. The position error for AOGL is plotted in Fig. 4(a) with an approximate maximum of 3, 6 and 9.5 m for a wind speed of 30, 40, 50% of the UAV airspeed. The NLGL performance, as shown in Fig. 4(b), deteriorates considerably in presence of high winds and corresponding maximum position errors are 14.5, 19 and 25 m, respectively.
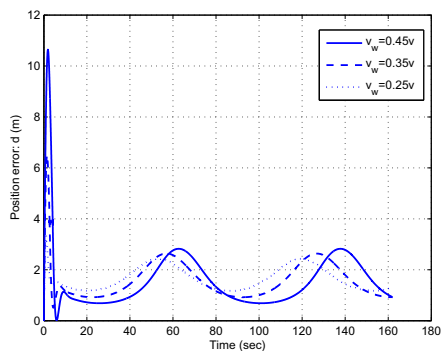
5.2 Circular path following

Next, we consider a circular path of radius 250 m centered at the origin and a UAV initially following the circle with no errors. The wind is considered blowing at a speed 30% of the UAV air speed in a direction perpendicular to the UAV initial heading. The trajectories are plotted in Fig. 5(a) where the blue and red color paths show AOGL and NLGL trajectories, respectively. The desired circular path is shown by a dashed curve. Again, the wind is less affective against the AOGL law where a maximum position error, as plotted in Fig. 5 (b), of 4.2 m in observed. The corresponding maximum error for NLGL is around 16 m. Note that the position errors do not converge to zero as in the straight line following case


(a) Trajectories
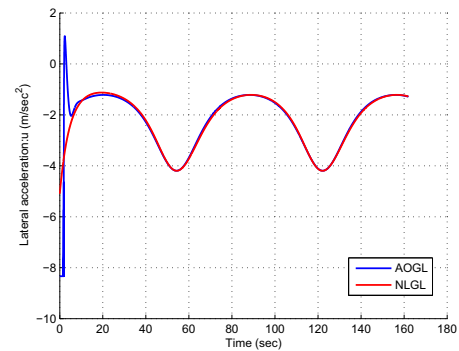
(b) Position error

(c) Lateral accelerations

Fig. 5. Circular path following in 30% wind

since the UAV would require a centripetal acceleration to follow the circular path and AOGL needs position and velocity errors to generate it. The corresponding lateral acceleration profiles, as plotted in Fig. 5(c), shows a higher initial control response by the AOGL resulting in superior error control. Next, we study the effect of wind magnitude on circular path following with wind speeds 25, 35 and 45 % UAV air speed. All other parameters are the same as previously. The position errors for AOGL are plotted in Fig.6 (a) with a maximum of 3.3, 6.2 and 10.4 m for $v_w = 0.25v$, $0.35v$, $45v$, respectively. The corresponding maximum error values for NLGL, as shown in Fig.6 (b), are 12.9, 18.1 and 25.2 m, respectively. A considerable position error improvement is gained using the proposed guidance law.

(a) Position error for AOGL
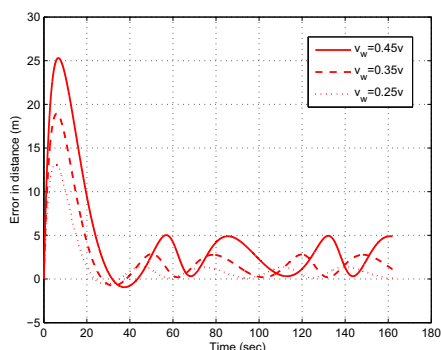
(b) Position error for NLGL

Fig. 6. Position error comparison in 25, 35 and 45 % wind following a circular path

6. CONCLUSIONS

An adaptive optimal UAV guidance law is presented for high wind flights. Infinite horizon LQR formulation is used to solve the guidance problem after linearizing the error dynamics. An adaptive state weighting matrix is used for tighter control of UAV errors in high disturbances. The guidance law results is considerably low errors as compared to an existing law in the literature. Simulations are carried out for wind speeds up to half the UAV airspeed for straight line and circular path following.

REFERENCES

S. Shehab and L. Rodrigues   Preliminary Results on UAV Path Following Using Piecewise-Affine Control   *Proceedings of the IEEE Conference on Control Applications*, Toronto, Canada, 2005, pp. 358-363 doi:10.1109/CCA.2005.1507151.

I. Kaminer, O. Yakimenko, A. Pascoal and R. Ghabcheloo   Path Generation, Path Following and Coordinated Control for Time Critical Missions of Multiple UAVs   *Proceedings of the American Control Conference*, Minneapolis, Minnesota, USA, 2006, pp. 4906-4913, doi:10.1109/ACC.2006.1657498

C. Cao and N. Hovakimyan, I. Kaminer, V.V. Patel and V. Dobrokhodov   Stabilization of Cascaded Systems via L1 Adaptive Controller with Application to a UAV Path Following Problem and Flight Test Results   *Proceedings of the American Control Conference*, New York, NY, USA, 2007, pp. 1787-1792, doi:10.1109/ACC.2007.4283028

D.R. Nelson, D.B. Barber, T.W. McLain and R.W. Beard Vector Field Path Following for Small Unmanned Air Vehicles *Proceedings of the American Control Conference*, Minneapolis, Minnesota, USA, 2006, pp. 5788-5794, doi:10.1109/ACC.2006.1657648

R. Rysdyk UAV Path Following for Constant Line-of-Sight *AIAA Unmanned Unlimited Systems, Technologies and Operations Aerospace, Land and Sea Conference*, San Diego, CA, USA, 2003, AIAA-2003-6626.

D.A. Lawrence, E.W. Frew and W.J. Pisano Lyapunov Vector Fields for Autonomous UAV Flight Control *AIAA Guidance, Navigation and Control Conference and Exhibit*, Hilton Head, South Carolina, USA, 2007, AIAA 2007-6317.

N. Ceccarelli, J.J. Enright, E.Frazzoli, S.J. Rasmussen and C.J. Schumacher Micro UAV Path Planning for Reconnaissance in Wind *Proceedings of the American Control Conference*, New York City, NY, USA, 2007, pp. 5310-5315, doi:10.1109/ACC.2007.4282479.

M. Breivik and T.I. Fossen Principles of Guidance-Based Path Following in 2D and 3D *Proceedings of the IEEE Conference on Decision and Control*, Seville, Spain, 2005, pp. 627-634, doi:10.1109/CDC.2005.1582226.

S. Park, J. Deystt and J.P. How Performance and Lyapunov Stability of a Nonlinear Path-Following Guidance Method *Journal of Guidance, Control, and Dynamics*, vol. 30, no. 6, pp. 1718-1728, doi:10.2514/1.28957.